



## Summative effects of vascular risk factors on cortical thickness in mild cognitive impairment



Ekaterina Tchistiakova<sup>a,b,c,\*</sup>, Bradley J. MacIntosh<sup>a,b,c</sup>, for the Alzheimer's Disease Neuroimaging Initiative<sup>1</sup>

<sup>a</sup> Department of Medical Biophysics, University of Toronto, Toronto, Ontario, Canada

<sup>b</sup> Heart and Stroke Foundation Canadian Partnership for Stroke Recovery, Toronto, Ontario, Canada

<sup>c</sup> Brain Sciences Research Program, Sunnybrook Research Institute, Toronto, Ontario, Canada

### ARTICLE INFO

#### Article history:

Received 23 September 2015

Received in revised form 11 May 2016

Accepted 11 May 2016

Available online 20 May 2016

#### Keywords:

Cortical thickness

Summative vascular risk factor index

Mild cognitive impairment

### ABSTRACT

Vascular risk factors (VRFs) increase the risk of Alzheimer's disease (AD) and contribute to neurodegenerative processes. The purpose of this study was to investigate whether increasing number of VRFs contributes to within-cohort differences in cortical thickness (CThk) among adults with mild cognitive impairment (MCI) and cognitively intact older controls from the AD Neuroimaging Initiative 1, GO, and 2 data sets. Multivariate partial least squares analysis was used to investigate the effect of VRF index on regional CThk measurements, which produced a significant latent variable and identified patterns of cortical thinning in the MCI group but not controls. Subsequent analyses tested the interaction effects between VRF index and cognitive grouping and examined 1-year follow-up data. There was evidence of a VRF index by cognitive group interaction. Partial least squares results were replicated at 1-year follow-up among MCI cohort in a subset of baseline CThk regions. This study provides evidence that a summative VRF index accounts for some of the variance in brain tissue loss in regions implicated in AD among MCI adults.

© 2016 Elsevier Inc. All rights reserved.

### 1. Introduction

Alzheimer's disease (AD) is a progressive neurodegenerative age-related disease characterized by increased accumulation of fibrillar  $\beta$ -amyloid ( $A\beta$ ) in neuritic and non-neuritic plaques in the cortex and striatum (Edison et al., 2008), extensive brain atrophy (Thompson et al., 2003), decreased glucose metabolism (Devanand et al., 2010), and debilitating cognitive decline (Becker et al., 1988). Amnesic mild cognitive impairment (MCI) is considered a prodromal stage of AD (Petersen et al., 1999), however, not all individuals with MCI develop AD. Consequently, several recent studies identified MCI subgroups that are at a higher risk of converting to AD using univariate and multivariate treatment of structural, cognitive, and cerebrospinal fluid (CSF) data

(Nettiksimmons et al., 2014; Spulber et al., 2013). These findings have prompted new questions about the underlying causes of MCI heterogeneity. For instance, vascular risk factors (VRFs) are known to increase the risk of AD as well as other dementias and increasingly recognized for their role in adversely affecting vascular and metabolic pathways synergistic with AD-related neurodegeneration (Clerici et al., 2012; Kivipelto et al., 2001; Luchsinger et al., 2005). VRFs affect on vascular function can compromise glucose and oxygen supply in a manner that is additive to disruption of vascular network caused by AD pathology. VRF-mediated pathophysiology is thought to interact synergistically with cerebral amyloid angiopathy, which would affect both inflow of nutrients and clearance of  $\beta$ -amyloid (Murray et al., 2011). Furthermore, nondemented individuals with VRFs have demonstrated changes in brain structure in regions that are closely related to AD (Hajjar et al., 2010; Last et al., 2007). The impact of VRFs on brain structure in the context of AD, however, is still unclear.

The primary objective of this study was to investigate the impact that the number of VRFs has on cortical thickness (CThk) in individuals with MCI and cognitively intact older adults (normal controls [NC]). Previous studies demonstrate an association between individual VRFs, diabetes, hypertension, history of smoking, and cortical thinning in multiple brain regions (Brundel et al., 2010;

\* Corresponding author at: Brain Sciences Research Program, Sunnybrook Research Institute, 2075 Bayview Avenue, Room M6 168, Toronto, ON M4N 3M5, Canada. Tel.: 1-416-480-6100 x 85407; fax: 1-416-480-4223.

E-mail address: [ekat@sri.utoronto.ca](mailto:ekat@sri.utoronto.ca) (E. Tchistiakova).

<sup>1</sup> Data used in preparation of this article were obtained from the Alzheimer's Disease Neuroimaging Initiative database ([adni.loni.usc.edu](http://adni.loni.usc.edu)). As such, the investigators within the ADNI contributed to the design and implementation of ADNI and/or provided data but did not participate in analysis or writing of this report. A complete listing of ADNI investigators can be found at: [http://adni.loni.usc.edu/wp-content/uploads/how\\_to\\_apply/ADNI\\_Acknowledgement\\_List.pdf](http://adni.loni.usc.edu/wp-content/uploads/how_to_apply/ADNI_Acknowledgement_List.pdf).

Gonzalez et al., 2015; Leritz et al., 2011). Most of these studies focused on the individual VRFs, i.e., examining the effect of one VRF while adjusting for other risk factors. This approach, however, may result in overadjustment and underestimation of the true VRF effects. Since VRFs seldom occur in isolation (Selby et al., 2004), using the combined VRF score is likely to improve sensitivity of detecting their effects on brain health. Several recent studies demonstrated the utility of aggregate VRF scores tested on structural and vascular brain measures (Bangen et al., 2014; De Toledo Ferraz Alves et al., 2011; Rondina et al., 2014; Tchistiakova et al., 2015).

VRFs affect a wide range of brain regions. For example, the effects of T2DM are most often detected within precuneus, posterior cingulate, entorhinal cortex, and middle temporal structures associated with memory (Brundel et al., 2010; Chen et al., 2015). Hypertension (HTN) has also been implicated in the effect on the temporal regions but appears to have an even more prominent impact on the prefrontal regions involved in executive function (Leritz et al., 2011). Finally, smoking is associated with a large scale of structural brain abnormalities including decreased gray matter density in prefrontal regions, cerebellum, precuneus, posterior cingulate, thalamus, and precentral gyri (Almeida et al., 2008; Brody et al., 2004). The reported spatial overlap between VRF-impacted regions and AD-related structural changes within temporal and frontal areas may lead to an enhanced vulnerability of these regions in individuals with both conditions. This overarching hypothesis serves as the main motivation for the present study.

Our goal was to examine whether increased VRF burden is related to the high degree of within-cohort structural variability in the group of older adults at risk for AD, i.e., MCI.

VRFs were combined into a summative VRF index (i.e., having 1, 2, or 3 VRFs). Whereas the literature on smoking, diabetes, and hypertension is unambiguous for their deleterious effects on brain structure, the same may not be the case for hypercholesterolemia since some report positive (Leritz et al., 2011; van Velsen et al., 2013) and others report negative (Walhovd et al., 2014) associations with CThk; therefore, it was not included in VRF index.

The impact of VRFs on CThk was assessed using multivariate partial least squares (PLS) analysis, which permits identification of distributed patterns of brain changes most related to a specific task or condition (Addis et al., 2004; Luk et al., 2010). This approach is efficient from a statistical point of view, useful at identifying latent patterns in the data, and often more sensitive than univariate techniques when dependent variables are correlated (McIntosh et al., 2004). Regional structural differences are often highly correlated; thus, PLS is well suited in this context. Furthermore, PLS may improve characterization of disease impact on the brain in conditions where effects are expected to involve multiple cortical and subcortical areas distributed throughout the brain by examining multiple regions at the same time (Khedher et al., 2015; Luk et al., 2010).

Our primary hypothesis in MCI adults is that it will be possible to use PLS to identify decreased CThk in relation to the summative VRF index. To support this primary analysis, we conduct an equivalent PLS analysis on CThk data among NC and consider follow-up CThk data from the MCI group. As part of the secondary analyses, we explore whether the influence of VRF index is different between cognitive groups. To test the theory that the VRF index and cognitive status work synergistically on CThk changes, our secondary hypothesis is that there will be an interaction effect of summative VRF index by cognitive group. Finally, we hypothesize that increasing VRF index may influence inter-regional CThk correlations. These correlations may either increase with VRF index, if 2 regions thin together as the VRF index increases, or decrease and even show negative association if there is localized degeneration. We hypothesize that the effect of VRF index on inter-regional

correlations will depend on the brain region. In particular, we expect temporal regions to show the highest disruption in correlations with other areas as these regions are known to be heavily impacted by both VRF and AD-related pathologies.

## 2. Materials and methods

### 2.1. AD Neuroimaging Initiative data set

The data used in this study were downloaded from the AD Neuroimaging Initiative (ADNI) database ([www.adni.loni.usc.edu](http://www.adni.loni.usc.edu)), launched in 2003 by the National Institute on Aging, the National Institute of Biomedical Imaging and Bioengineering, the Food and Drug Administration, private pharmaceutical companies, and nonprofit organizations as a 5-year private–public partnership. The primary goal of ADNI has been to test whether serial magnetic resonance imaging (MRI), positron emission tomography and other biological markers, and clinical and neuropsychological assessment can be combined to measure the progression of MCI and early AD. Determination of sensitive and specific markers of very early AD progression is intended to aid researchers and clinicians to develop new treatments and monitor their effectiveness, as well as lessen the time and cost of clinical trials. The Principal Investigator of this initiative is Michael W. Weiner, MD, VA Medical Center and University of California, San Francisco. ADNI is the result of efforts of many coinvestigators from a broad range of academic institutions and private corporations, and subjects have been recruited from over 50 sites across the United States and Canada.

### 2.2. Participants

Participants were enrolled in ADNI if they were between 55- and 90-year old, spoke English or Spanish as their first language and completed at least 6 years of schooling. Diagnostic classification was made by ADNI investigators using established criteria for NC, early MCI, late MCI, or early stages of AD (McKhann, Drachman and Folstein, 1984; McKhann et al., 2011; Petersen et al., 1999). Controls had mini-mental status examination scores between 24 and 30 and no significant memory concerns. MCI adults had mini-mental status examination scores between 24 and 30; memory complaint; objective memory loss as quantified by the Wechsler Memory Scale Logical Memory II test; a Clinical Dementia Rating score of 0.5; lack of cognitive impairment in other domains such as executive function, visuospatial function and language; relative sparing of activities of daily living; and absence of frank dementia.

The present study included early and late MCI individuals as well as the NC group, all of whom had a baseline MRI scan. MRI data were collected on 1.5 T and 3 T MRI scanners in accordance with a standardized protocol (Jack et al., 2008). A typical protocol for T1-weighted 3D-MPRAGE sequence included: repetition time/echo time/inversion time = 2300/2.9/900 ms, matrix = 256 × 240 × 192, voxel size = 1 × 1 × 1.2 mm<sup>3</sup>, number of slices = 160, and flip angle = 9°. Follow-up MRI data were also obtained at 1 year for a subset of MCI participants.

In addition to imaging data, participants' demographics including systolic and diastolic blood pressure (SBP and DBP), fasting blood glucose levels, and Apolipoprotein E (APOE) genotype were obtained. Participants were included in the final analyses if they had at least 1 VRF (diabetes, prehypertension/hypertension, and history of smoking) and were assigned into subgroups based on the summative VRF index (i.e., 1, 2, or 3). The presence of VRF was established based on the medications associated with the treatment of that VRF and/or the condition was listed in the medical notes of the recent medical history. In addition, measures of blood pressure (SBP ≥ 130 mm Hg and/or DBP ≥ 85 mm Hg; Chobanian

et al., 2003; Haight et al., 2015) and fasting blood glucose ( $\geq 126$  mg/dL; American Diabetes Association, 2011) were used as part of the classification for prehypertension/hypertension and diabetes, respectively, to account for potential undiagnosed VRFs. Smoking was classified as “yes” if participants had a history of smoking at any time based on the previous evidence of the effects of midlife smoking on brain structure (DeBette et al., 2011).

### 2.3. Image analysis

T1-weighted high-resolution images from ADNI database were preprocessed by the University of California, San Francisco Medical Centre using FreeSurfer software (V5.1, <http://surfer.nmr.mgh.harvard.edu/>) described in more details elsewhere (Dale, Fischl and Sereno, 1999). Briefly: (1) T1-weighted images were motion corrected and averaged across multiple volumetric images (Reuter, Rosas and Fischl, 2010), (2) all nonbrain structures were removed (Ségonne et al., 2004), (3) images were transformed into Talairach space, (4) subcortical white and deep gray matters volumetric structures were segmented and intensity normalization applied (Fischl et al., 2002; Sied, Zijdenbos and Evans, 1998), (5) gray/white matter boundary was covered with triangular tessellation and a deformation algorithm applied to produce a final representation of the boundary between gray and white matter as well as the gray matter/CSF boundary, (6) finally, cortical parcellation was performed and regional structural statistics estimated, i.e., CThk and cortical volumes (Fischl et al., 2002). CThk was computed as the closest distance between gray/white and gray/CSF surfaces for 34 regions for right and left hemispheres (Fischl and Dale, 2000) and are available for download from the ADNI website. A visual quality control of automated FreeSurfer segmentation was also performed. Only CThk measures for images that passed segmentation quality control in frontal, temporal, parietal, occipital lobes, and insula were included in this study.

#### 2.3.1. Assessment of summative VRF index impact on CThk with PLS

Comparison of VRF index subgroups was performed using PLS on 68 CThk regions produced by FreeSurfer segmentation for MCI and NC groups separately. Before PLS analysis, a linear model was used to regress the effects of age, gender, APOE status (0 = no  $\epsilon 4$  alleles, 1 = one or more  $\epsilon 4$  alleles) and MRI field strength for each cortical region. This strategy of adjusting CThk values was designed to restrict PLS analysis to structural differences driven by VRF index and has been previously used in multivariate analyses (He et al., 2008). The PLS pipeline was developed at Baycrest Hospital, Rotman Research Institute, implemented using Matlab software and is described in more details elsewhere (McIntosh et al., 1996; McIntosh and Lobaugh, 2004;). Briefly: (1) a cross-correlation matrix was computed between the design and data matrices (e.g., VRF index subgroup vs. regional CThk measures), (2) a singular value decomposition was applied to the cross-correlation matrix to generate a set of orthogonal latent variables (LVs) containing a pair of singular images (design matrix and salience matrix) and the corresponding singular values (covariance between the 2 matrices), (3) finally, brain scores were computed as the dot product of the salience matrix and the original data matrix (McIntosh et al., 1996, 2004).

Statistical assessment of the LVs is done using permutation testing for the LV significance and bootstrap resampling for region localization. In the first case, permutations are used to establish if any or all of the LVs are statistically significant by randomly reordering the rows of the design matrix and computing a new set of LVs each time. The singular values of these LVs are then compared with that of the original LV, and the probability is assigned to the original LV value based on the number of times the statistic from

the permuted LVs exceeds the original value (McIntosh et al., 1996). Saliences are weights that determine how strongly each voxel (here, CThk region) contributes to the identified LV. To determine the reliability of the saliencs for CThk regions characterizing the LV pattern, a bootstrap resampling is used on the salience matrix, estimating the standard error of voxel saliencs within that LV. The ratio of saliencs to standard errors is referred to as the bootstrap ratio (BSR; McIntosh et al., 2004). Since both permutation and bootstrapping are performed on the entire LV pattern no additional multiple comparison correction is required (McIntosh et al., 2004).

Adjusted regional CThk measures were formatted as 2D images making data conducive to the PLS software, namely CThk values were assigned to 68 voxels in an image for each participant. Individuals' data were then combined into a single matrix based on the VRF index, where each row corresponded to a single participant and each column contained regional CThk measures. Next, PLS was performed to produce a set of LVs, thereby identifying inherent association patterns between CThk and VRF index. Permutation testing with 1500 permutations ( $p < 0.05$  for significance) was performed to determine the significance of each LV, followed by a bootstrap resampling with 500 bootstraps to identify brain regions that consistently showed the significant LV pattern (BSR  $> 2.0$  for significance) and to generate a 95% confidence intervals (CIs) for VRF index subgroup comparison.

#### 2.3.2. Effect of cognitive group X VRF index interaction on CThk

In the secondary analyses, we tested for a main effect of VRF index and cognitive group X VRF index interaction effect using an analysis of covariance (ANCOVA) in SPSS (version 21, IBM Corp., IMB SPSS Statistics for Mac, Armonk, NY, USA) in the regions identified by PLS. These analyses included both NC and MCI groups. CThk was adjusted for age, gender, APOE status, and MRI field strength. Correction for multiple comparisons was performed using the false discovery rate (FDR) method ( $q < 0.05$  for significance).

#### 2.3.3. Inter-regional CThk correlations

Inter-regional correlation matrices were computed for each VRF index subgroup by calculating correlation coefficients between CThk measures for every pair of regions identified by PLS. Correlation coefficients were then converted into z-values using Fisher's transform, and VRF index sub-groups were compared in a pairwise manner. Results were adjusted for multiple comparisons using FDR ( $q < 0.05$  for significance). Similarly to PLS analysis, adjusted CThk values (i.e., not the raw CThk values) were used in this correlation analysis.

#### 2.3.4. Replication sample using 1-year follow-up MRI

Effects of VRF index on CThk were examined in the regions identified in baseline PLS findings using the subset of MCI participants with available 1-year follow-up. An ANCOVA model that included age, gender, APOE status, and MRI field strength was used in SPSS (version 21, IBM Corp., IMB SPSS Statistics for Mac). VRF index subgrouping was preserved from baseline analysis as the initial classification was based on the medical history from all visits. Results were adjusted for multiple comparisons using FDR ( $q < 0.05$  for significance).

#### 2.3.5. Statistical analysis

Statistical comparison of VRF index subgroups in terms of demographics and clinical characteristics was performed using SPSS (version 21, IBM Corp., IMB SPSS Statistics for Mac). Age, SBP, DBP, fasting blood glucose, body mass index, white matter hyperintensities volumes, and CSF measures were not normally distributed and were, therefore, compared using nonparametric Kruskal–Wallis test. Categorical variables were compared using  $\chi^2$  test.

### 3. Results

#### 3.1. Participants

T1-weighted MRI data were preprocessed for 1437 participants (532 NC and 905 MCI), of which 383 and 672 passed segmentation quality control for NC and MCI, respectively (see Fig. 1). For NC, 354 of 383 had a VRF index of one or more. For MCI, 604 of 672 had a VRF index of one or more. Since APOE status was included as a covariate in all analyses, 11 NC and 28 MCI participants with missing genotype data were excluded. Final analysis included 343 NC (VRF index 1, 196; VRF index 2, 131; and VRF index 3, 16) and 576 MCI (VRF index 1, 311; VRF index 2, 234; and VRF index 3, 31).

Diagnosis of preHTN/HTN was made based on either medical history/medications ( $N = 162$ ), a high BP reading ( $N = 242$ ), or both ( $N = 412$ ). Similarly, diabetes mellitus diagnosis was based on either medical history/medications ( $N = 83$ ), a high fasting glucose reading ( $N = 42$ ), or both ( $N = 38$ ). Participants' demographics are summarized in Table 1.

Fasting blood glucose levels were significantly different between VRF index subgroups in both NC and MCI ( $p = 0.002$  and  $p < 0.001$ , respectively), with a higher VRF index being associated with higher fasting glucose. SBP and body mass index were also significantly different between VRF index subgroups in MCI ( $p = 0.01$  and  $p < 0.001$ , respectively). No significant differences were detected between VRF index subgroups in any other measures.

#### 3.2. Impact of summative VRF index on CThk

PLS analysis of CThk data in the MCI cohort produced one significant LV ( $p = 0.01$ ) that explained 95.3% of the covariance between adjusted CThk and the VRF index. Contributions of each group to this pattern and pairwise subgroup differences were determined using 95% CI bars from bootstrap testing. All 3 VRF index subgroups contributed significantly to the identified pattern (i.e., CIs did not overlap with 0). The LV showed a stepwise pattern with increasing VRF index, i.e., higher VRF index was associated with lower brain scores (which in this study correspond to

weighted CThk measures; see Fig. 2A). Significant subgroup differences were observed between VRF index 1 and VRF index 3 subgroups and between VRF index 2 and VRF index 3 subgroups (i.e., non-overlapping CIs) but not between VRF index 1 and VRF index 2 subgroups. This LV pattern was reliably detected (i.e.,  $BSR \geq 2.0$ ) in the (1) bilateral-entorhinal cortex, pars orbitalis, and lateral orbitofrontal regions; (2) right-parahippocampal, inferior temporal, medial orbitofrontal, rostral middle frontal, and frontal pole regions; and (3) left insula and temporal pole (see Fig. 2B). Our secondary PLS analysis on the NC group did not produce any significant LVs that would explain VRF index differences ( $p = 0.4$ ).

#### 3.3. Effect of cognitive group X VRF index interaction on CThk

The results of the ANCOVA analysis revealed a main effect of VRF index across 2 cognitive groups in the right frontal pole ( $p = 0.01$ ) and left lateral orbitofrontal region ( $p = 0.02$ ). An interaction between cognitive diagnosis and VRF index was observed in right medial orbitofrontal ( $p = 0.001$ ) and right parahippocampal ( $p = 0.04$ ) regions, where the impact of VRF index was seen in the MCI but not NC group. Results are summarized in Fig. 3. Only the interaction term in the right medial orbitofrontal region survived FDR correction.

#### 3.4. Inter-regional CThk correlations

The inter-regional CThk correlation matrices by VRF index subgroups in the MCI group are shown in Fig. 4A. Groups with VRF index of 1 and 2 had positive inter-regional correlations between all examined regions. By contrast, the group with a VRF index of 3 had several negative correlations, primarily with right and left entorhinal cortices. Pairwise comparisons revealed significant ( $p < 0.05$  FDR-corrected) between VRF index subgroup differences. The scatter plots for these correlations are included in Fig. 4B.

#### 3.5. Replication results using 1-year follow-up MRI

One year follow-up MRI data were available for 328 MCI participants (VRF index 1, 178; VRF index 2, 138; VRF index 3, 12). Of the 13 regions identified in the baseline PLS findings, 3 showed significant association with VRF index at follow-up: right inferior temporal region ( $p = 0.001$ ), right entorhinal cortex ( $p = 0.02$ ), and right parahippocampal ( $p = 0.05$ ). The right inferior temporal region remained significant after FDR correction. A post hoc analysis revealed a significant decrease in CThk in all 3 regions in the group with VRF index of 3 compared with VRF index of 1 (right inferior temporal:  $p < 0.001$ , right entorhinal:  $p = 0.02$ , right parahippocampal:  $p = 0.04$ ), and VRF index 2 group (right inferior temporal:  $p = 0.001$ , right entorhinal:  $p = 0.006$ , right parahippocampal:  $p = 0.02$ ) but not between VRF index of 1 and 2 ( $p > 0.05$ ). The results of the follow-up analysis are demonstrated in Supplementary Fig. 1. The data for HC in the same 13 regions was included for comparison. Similarly to the baseline, no VRF index subgroup effects were detected in HC group at follow-up.

### 4. Discussion

This study reveals there are significant associations between the summative VRF index and CThk in the temporal and frontal regions among older adults with MCI who have at least one VRF. No such VRF patterns of cortical thinning were seen when the NC group was treated separately; however, a main effect of VRF index across the cognitive cohorts was found in the left lateral orbitofrontal and right frontal pole regions and a significant cognitive group by VRF index interaction effect was observed in the right medial

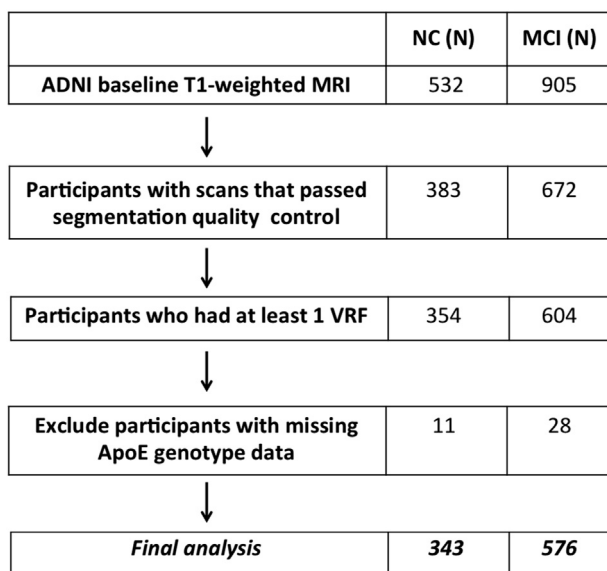


**Fig. 1.** Flowchart of participants included in CThk analysis. Abbreviations: ADNI, Alzheimer's Disease Neuroimaging Initiative; CThk, cortical thickness; MCI, mild cognitive impairment; MRI, magnetic resonance imaging; NC, normal controls; VRF, vascular risk factors.

**Table 1**  
Participants demographics

|                                  | NC           |              |              |                | <i>p</i> value | MCI          |              |             |                |
|----------------------------------|--------------|--------------|--------------|----------------|----------------|--------------|--------------|-------------|----------------|
|                                  | VRF index 1  | VRF index 2  | VRF index 3  | <i>p</i> value |                | VRF index 1  | VRF index 2  | VRF index 3 | <i>p</i> value |
| N                                | 196          | 131          | 16           |                | 311            | 234          | 31           |             |                |
| Age (y)                          | 73.7 ± 5.8   | 74.7 ± 5.4   | 74.3 ± 5.1   | NS             | 72.2 ± 7.3     | 72.8 ± 7.2   | 72.9 ± 6.4   | NS          |                |
| Race (W/B/O)                     | 177/12/7     | 117/11/3     | 15/1/0       | NS             | 294/9/8        | 209/13/12    | 29/1/1       | NS          |                |
| Gender (F)                       | 204          | 65           | 4            | NS             | 135            | 102          | 9            | NS          |                |
| Apolipoprotein E (ε4 ≥ 1 allele) | 56           | 37           | 4            | NS             | 158            | 120          | 15           | NS          |                |
| Aβ (pg/mL)                       | 198.8 ± 50.1 | 204.6 ± 54.6 | 215.2 ± 56.0 | NS             | 173.6 ± 51.9   | 173.9 ± 49.9 | 179.0 ± 57.6 | NS          |                |
| Tau (pg/mL)                      | 63.8 ± 31.7  | 68.4 ± 32.0  | 66.6 ± 24.5  | NS             | 88.6 ± 55.2    | 83.0 ± 47.8  | 82.3 ± 49.5  | NS          |                |
| Ptau (pg/mL)                     | 31.0 ± 15.7  | 32.8 ± 15.6  | 36.6 ± 11.9  | NS             | 41.9 ± 26.6    | 40.9 ± 22.0  | 36.8 ± 22.4  | NS          |                |
| Systolic BP (mm Hg)              | 134.8 ± 16.4 | 139.0 ± 16.9 | 135.2 ± 10.3 | NS             | 135.0 ± 16.5   | 139.5 ± 17.1 | 137.0 ± 15.5 | 0.01        |                |
| Diastolic BP (mm Hg)             | 75.3 ± 10.4  | 75.9 ± 9.8   | 74.9 ± 7.6   | NS             | 75.8 ± 9.5     | 75.8 ± 10.0  | 75.2 ± 11.1  | NS          |                |
| Fasting blood glucose (mg/dL)    | 96.9 ± 14.0  | 103.7 ± 22.7 | 121.7 ± 34.2 | 0.002          | 94.7 ± 11.9    | 103.9 ± 25.1 | 130.0 ± 64.0 | <0.001      |                |
| BMI                              | 26.7 ± 3.9   | 27.7 ± 4.8   | 29.3 ± 5.4   | NS             | 26.8 ± 4.8     | 27.6 ± 5.1   | 30.0 ± 4.9   | <0.001      |                |
| WMH ICV normalized (cc)          | 2.4 ± 3.8    | 2.6 ± 5.1    | 2.9 ± 7.0    | NS             | 3.3 ± 6.7      | 2.9 ± 4.2    | 4.0 ± 7.0    | NS          |                |
| DM                               | 7            | 35           | 16           |                | 10             | 64           | 31           |             |                |
| preHTN/HTN                       | 159          | 127          | 16           |                | 253            | 230          | 31           |             |                |
| Smoking history                  | 30           | 100          | 16           |                | 48             | 174          | 31           |             |                |

Data are mean ± SD.

Aβ measurements were missing for: 161 NC (VRF index 1, 92; VRF index 2, 60; and VRF index 3, 9) and 250 MCI (VRF index 1, 134; VRF index 2, 101; and VRF index 3, 15). Tau measurements were missing for: 165 NC (VRF index 1, 96; VRF index 2, 60; and VRF index 3, 9) and 261 MCI (VRF index 1, 139; VRF index 2, 107; and VRF index 3, 15). Ptau measurements were missing for: 161 NC (VRF index 1, 92; VRF index 2, 60; and VRF index 3, 9) and 250 MCI (VRF index 1, 134; VRF index 2, 101; and VRF index 3, 15). Fasting blood glucose measures were missing for: 28 NC (VRF index 1, 8; VRF index 2, 19; and VRF index 3, 1) and 10 MCI (VRF index 1, 7; VRF index 2, 1; and VRF index 3, 2). BMI measurements were missing for: 4 NC (VRF index 1, 2; VRF index 2, 2).

WMH volumes were missing for: 19 NC (VRF index 1, 5 and VRF index 2, 14) and 11 MCI (VRF index 1, 5; VRF index 2, 5; and VRF index 3, 1).

Key: Aβ, β amyloid; B, black; BMI, body mass index; BP, blood pressure; DM, diabetes mellitus; HTN, hypertension; ICV, intracranial volume; MCI, mild cognitive impairment; NC, normal controls; O, other; Ptau, phosphorylated tau; Tau, total tau; VRF, vascular risk factors; W, white; WMH, white matter hyperintensities.

orbitofrontal and right parahippocampal regions. Increased VRF index was also associated with differences in inter-regional CThk correlations between left and right entorhinal cortices and several frontal regions. Follow-up CThk data in a subset of the MCI sample confirmed the impact of increasing VRF index on CThk in 3 temporal regions identified at baseline.

The novelty of the present study is in the use of a multivariate PLS analysis to identify regions where reduced CThk was explained by the summative VRF index. This PLS approach interrogated all 68 CThk regions simultaneously and inherently accounted for collinearity of the dependent variables. PLS is thus an efficient and prudent strategy of characterizing between-subject differences in CThk. Furthermore, the Rotman PLS software is also statistically rigorous because of the permutation and bootstrap steps that are designed to assess the robustness of the LV and the individual CThk regions. Only one significant LV was found in the MCI group, of which case each of the VRF subgroups contributed to this LV in a “stair-case” pattern (i.e., higher VRF index corresponded to lower

CThk). Identified regions included some of the regions previously seen impacted by the individual VRFs. For example, several previous studies have shown associations between cortical thinning within temporal regions and T2DM (Brundel et al., 2010; Chen et al., 2015), temporal and frontal regions and HTN (Leritz et al., 2011) and preferential effect of smoking on cortical structure in frontal regions (Almeida et al., 2008; Brody et al., 2004). Our findings are also consistent with earlier studies using an aggregate vascular score, i.e., the Framingham Cardiovascular Risk Profile, which demonstrate negative associations between vascular burden and temporal (Cardenas et al., 2012; Villeneuve et al., 2014) and frontal (Villeneuve et al., 2014) CThk in older NC and MCI adults. VRF-sensitive regions identified by PLS showed a high degree of overlap with cortical thinning patterns within frontotemporal areas characteristic of AD (Thompson et al., 2003). These findings support our hypothesis that there are regions that are vulnerable to both AD and VRF-related neurodegeneration, possibly through synergistic effects of vascular dysfunction and AD-specific pathophysiology,

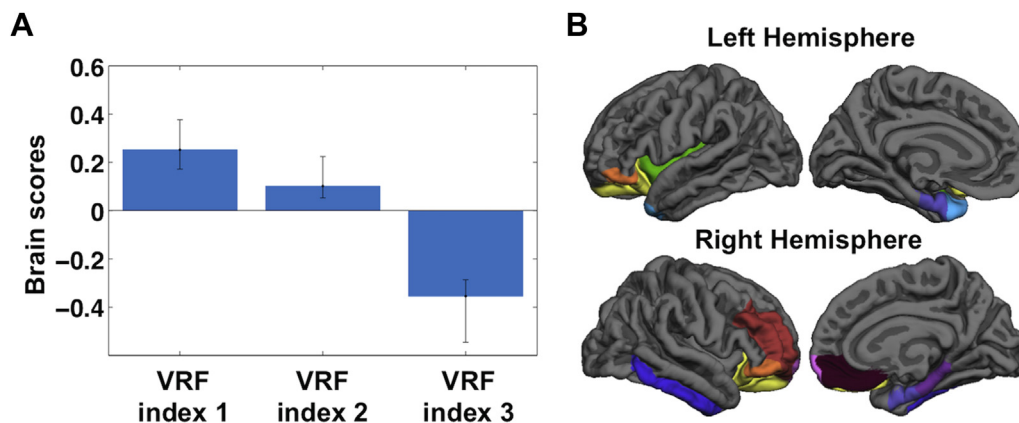


**Fig. 2.** (A) Significant LV pattern for PLS on CThk versus summative VRF index in MCI cohort. Error bars represent 95% confidence intervals generated using bootstrap testing. (B) Regions exhibiting the LV pattern. Abbreviations: CThk, cortical thickness; LV, latent variable; MCI, mild cognitive impairment; PLS, partial least squares; VRF, vascular risk factors.

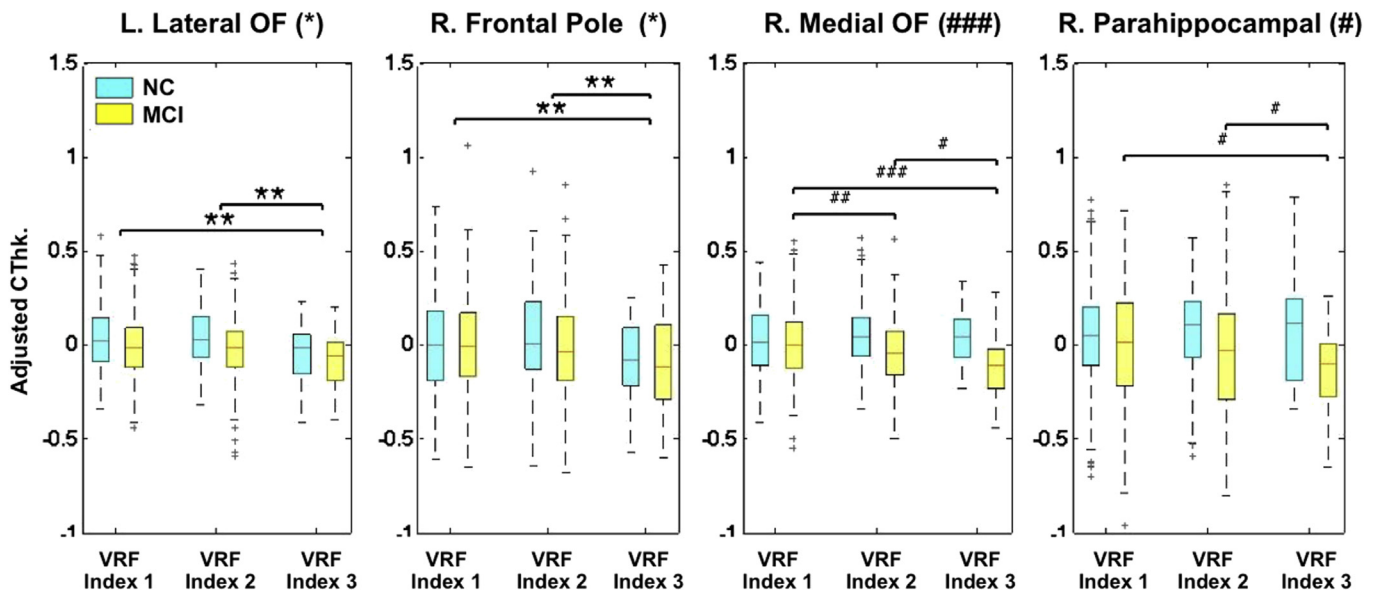


**Fig. 3.** Main effects of VRF index (\* indicates  $p < 0.05$ , \*\* indicates  $p < 0.01$ ) and cognitive group X VRF index interaction (# indicates  $p < 0.05$ , ## indicates  $p < 0.01$ , ### indicates  $p \leq 0.001$ ). Also shown are the post hoc between VRF index subgroup comparisons. For regions showing a significant interaction term, the post hoc test compares the CThk between VRF index sub-groups within the MCI cohort. Abbreviations: CThk, cortical thickness; OF, orbitofrontal; VRF, vascular risk factors.

such as A $\beta$  accumulation. The findings also suggest that VRFs contribute to heterogeneity in structural neuroimaging data within MCI.

VRF index was also found to influence inter-regional CThk correlations in the MCI cohort. Negative correlations were observed between bilateral entorhinal cortices and several frontal regions in the group with 3 VRFs. Changes in the inter-regional CThk correlations were previously observed in the AD individuals compared with NC (He et al., 2008), where negative correlations between brain regions were attributed to regional disconnectivity and/or localized degeneration (Alexander-Bloch et al., 2013).

The impact of VRFs on the brain is multifactorial, including structural degeneration of gray and white matter, cerebrovascular dysfunction and functional network reorganization (Hajjar et al., 2010; Last et al., 2007; Leritz et al., 2011; Musen et al., 2012). In the context of AD, VRFs contribute additively to vascular dysfunction, which appears to increase the risk of AD onset and progression through a “two-hit vascular hypothesis” (Zlokovic, 2011). “Hit one” is attributed to the accumulation of neurotoxic molecules and capillary hypoperfusion, which leads to the neuronal dysfunction. “Hit two” is the additional VRF-related vascular dysfunction that contributes to increased productions and decreased clearance of A $\beta$ . In the case of T2DM, this VRF may also directly contribute to A $\beta$  accumulation by decreasing the availability of insulin degrading enzyme, which is responsible for A $\beta$  clearance (Zhao et al., 2004). The processes of VRF brain impact are often interconnected, such that vascular dysfunction may decrease supply of oxygen and nutrients to brain tissues, contributing to cortical thinning (Alosco et al., 2014). CThk was chosen in this study as it has been shown to be a sensitive structural biomarker for detecting the effects of VRF and early signs of AD (Brundel et al., 2010; Leritz et al., 2011; Sabuncu et al., 2011). Structural imaging, used for CThk measurement, is also the most commonly used modality in neuroimaging, which facilitates the translations of current findings to other populations and increases the ease of result replication. Other metrics such as perfusion and white matter tractography may provide additional information on the mechanisms that could contribute to these structural changes. For example, a recent study by Maillard et al. (2015) demonstrated a significant impact of VRFs on white

matter fractional anisotropy, which was found to be reduced in individuals with  $\geq 2$  VRFs compared with those with only 1 VRF in a range of white matter tracts including the cingulum and uncinate fasciculus that connect temporal and frontal brain regions. Unlike the structural measures, however, white matter and perfusion imaging are rarely used in clinical protocols, and have only recently been added to ADNI, limiting the number of available data. These measures were, therefore, not considered in the present study but could be explored in future work.

Another important finding of this study is that we identified CThk regions that were associated with the VRF index in PLS analysis among MCI but not the NC cohort, which suggests a few things. First, the VRF index may have a larger effect size in MCI because this group is more susceptible to neurodegeneration. Second, there may be inherent biases in our selection of MCI and NC, namely the breakdown of VRF index subgroups. No attempts were made to match cognitive groups since our primary objective was to characterize the impact of VRF index in MCI. Third, VRFs may act synergistically with AD pathology in the MCI group, which served to reinforce our VRF index/CThk associations. A post hoc analysis on the selected PLS regions across the 2 cohorts showed a significant cognitive group by VRF index interaction in the right medial orbitofrontal and right parahippocampal regions. These results are consistent with a study on the interaction of VRFs and A $\beta$  deposition (a hallmark of AD) that observed thinner frontotemporal cortical regions in individuals with higher number of VRFs (Villeneuve et al., 2014). Finally, our attempt to replicate the baseline findings produced mixed results in the sense that only a subset of the PLS findings were detected at the 1-year follow-up, including the right entorhinal, right parahippocampal, and right inferior temporal regions. This may be due to the smaller sample available at follow-up, i.e., 328 samples versus 604 baseline samples. Of note, the replication findings were specific to the right temporal lobe, which may be an indication of persistent vulnerability of these brain regions to the VRF effects. These temporal findings are consistent with previous studies on hypertension and diabetes (Brundel et al., 2010; Leritz et al., 2011). The present study adds on to this literature by demonstrating the detrimental CThk effect of summative VRFs in these regions.

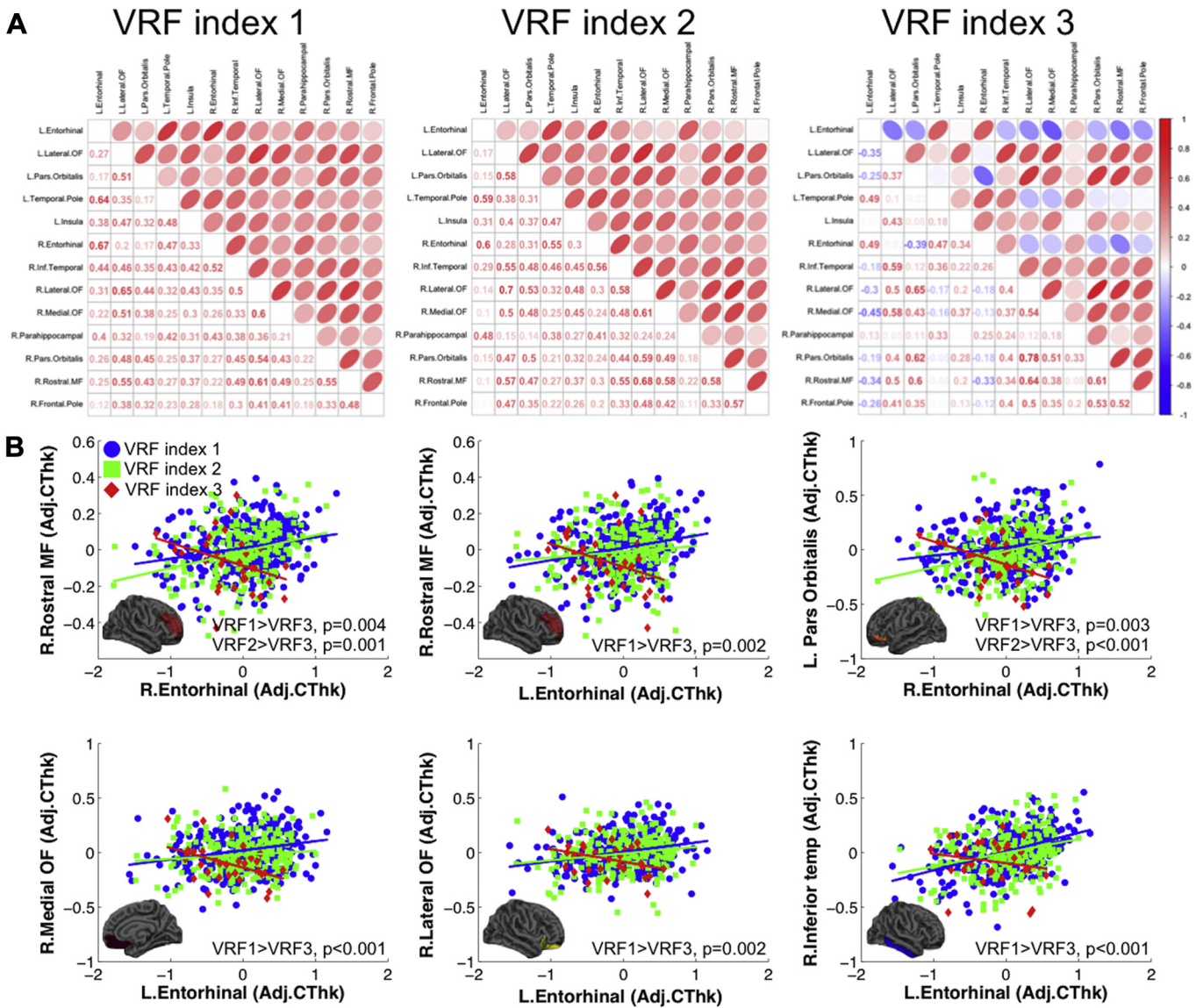


**Fig. 4.** (A) CThk region-by-region correlation coefficient maps shown for each of the VRF index subgroups; (B) scatter plots for regions with significant pairwise correlation differences between VRF subgroups ( $p < 0.05$ , FDR-corrected). Abbreviations: CThk, cortical thickness; FDR, false discovery rate; MF, middle frontal; OF, orbitofrontal; VRF, vascular risk factors.

Several limitations of this study need to be mentioned. First, we did not control for depression, previous cardiovascular and cerebrovascular events, which may have influenced our findings. Second, we used clinical diagnosis of NC and MCI to classify participants and did not include CSF levels of A $\beta$  and tau measurements in the analyses because of their limited availability at the time of this study (i.e., 53% of NC and 56% of MCI group had CSF samples). Future studies could examine their interaction with summative VRF index. Finally, we demonstrate that there is value in using a summative VRF index; this was a parsimonious approach to the complex effects of each of the VRFs. Adopting a more specific VRF model would likely be more informative, but there are 7 possible unique VRF subgroupings, which was simply not feasible at this time due to the required sample size per VRF subgroup. The VRF subgroups with an index of 3 were already small samples, namely 16 adults for NC and 31 adults for MCI. Fortunately, our PLS procedure include permutations to assess the level of significance for the LV identified in the MCI group. Although the summative VRF

index produced plausible CThk findings, future work could focus on different VRF models, be they categorical or continuous as a means to better characterize VRF interaction effects.

In conclusion, this study demonstrates the utility of PLS as a means to identify VRF-sensitive brain regions. A higher VRF index was associated with reduced CThk in the MCI cohort, a result that was partially reproduced in a smaller subset of 1-year follow-up data. We failed to detect a VRF index effect on CThk in the NC group, although a main VRF index effect was seen in 2 frontal regions when the 2 cognitive groups were combined. We also observed changes in the inter-regional CThk correlations between temporal and frontal brain regions in the subgroup with VRF index of 3 compared with VRF index of 1 and 2 subgroups. Overall, our findings suggest that the use of a summative VRF index is a well-suited strategy designed to characterize the comorbid diseases that influence neurodegeneration, and this treatment was particularly revealing when considering CThk heterogeneity in the MCI cohort.

## Disclosure statement

The authors have no conflicts of interest to disclose.

## Acknowledgements

This study was funded by the Canadian Institutes of Health Research (CIHR CSE133351). Data collection and sharing for this project was funded by the ADNI (National Institutes of Health Grant U01 AG024904) and DOD ADNI (Department of Defense award number W81XWH-12-2-0012). ADNI is funded by the National Institute on Aging, the National Institute of Biomedical Imaging and Bioengineering, and through generous contributions from the following: AbbVie, Alzheimer's Association; Alzheimer's Drug Discovery Foundation; Araclon Biotech; BioClinica, Inc; Biogen; Bristol-Myers Squibb Company; CereSpir, Inc; Eisai Inc; Elan Pharmaceuticals, Inc; Eli Lilly and Company; EuroImmun; F. Hoffmann-La Roche Ltd and its affiliated company Genentech, Inc; Fujirebio; GE Healthcare; IXICO Ltd; Janssen Alzheimer Immunotherapy Research & Development, LLC; Johnson & Johnson Pharmaceutical Research & Development LLC; Lumosity; Lundbeck; Merck & Co, Inc; Meso Scale Diagnostics, LLC; NeuroRx Research; Neurotrack Technologies; Novartis Pharmaceuticals Corporation; Pfizer Inc; Piramal Imaging; Servier; Takeda Pharmaceutical Company; and Transition Therapeutics. The Canadian Institutes of Health Research is providing funds to support ADNI clinical sites in Canada. Private sector contributions are facilitated by the Foundation for the National Institutes of Health ([www.fnih.org](http://www.fnih.org)). The grantee organization is the Northern California Institute for Research and Education, and the study is coordinated by the Alzheimer's Disease Cooperative Study at the University of California, San Diego. ADNI data are disseminated by the Laboratory for Neuro Imaging at the University of Southern California. The authors thank Dr. Walter Swardfager for useful discussion.

## Appendix A. Supplementary data

Supplementary data related to this article can be found online at <http://dx.doi.org/10.1016/j.neurobiolaging.2016.05.011>.

## References

- Addis, D.R., McIntosh, A.R., Moscovitch, M., Crawley, A.P., McAndrews, M.P., 2004. Characterizing spatial and temporal features of autobiographical memory retrieval networks: a partial least squares approach. *NeuroImage* 23, 1460–1471.
- Alexander-Bloch, A., Giedd, J.N., Bullmore, E., 2013. Imaging structural co-variance between human brain regions. *Nat. Rev. Neurosci.* 14, 322–336.
- Almeida, O.P., Garrido, G.J., Lautenschlager, N.T., Hulse, G.K., Jamrozik, K., Flicker, L., 2008. Smoking is associated with reduced cortical regional gray matter density in brain regions associated with incipient Alzheimer disease. *Am. J. Geriatr. Psychiatry* 16, 92–98.
- Alosco, M.L., Gunstad, J., Xu, X., Clark, U.S., Labbe, D.R., Riskin-Jones, H.H., Sweet, L.H., 2014. The impact of hypertension on cerebral perfusion and cortical thickness in older adults. *J. Am. Soc. Hypertens.* 8, 561–570.
- American Diabetes Association, 2011. Diagnosis and classification of diabetes mellitus. *Diabetes Care* 34 (Suppl. 1), S62–S69.
- Bangen, K.J., Nation, D.A., Clark, L.R., Harmell, A.L., Wierenga, C.E., Dev, S.I., Bondi, M.W., 2014. Interactive effects of vascular risk burden and advanced age on cerebral blood flow. *Front. Aging Neurosci.* 6, 159.
- Becker, J.T., Huff, F.J., Nebes, R.D., Holland, A., Boller, F., 1988. Neuropsychological function in Alzheimer's disease. pattern of impairment and rates of progression. *Arch. Neurol.* 45, 263–268.
- Brody, A.L., Mandelkern, M.A., Jarvik, M.E., Lee, G.S., Smith, E.C., Huang, J.C., London, E.D., 2004. Differences between smokers and nonsmokers in regional gray matter volumes and densities. *Biol. Psychiatry* 55, 77–84.
- Brundel, M., Van Den Heuvel, M., De Bresser, J., Kappelle, L.J., Biessels, G.J., 2010. Cerebral cortical thickness in patients with type 2 diabetes. *J. Neurol. Sci.* 299, 126–130.
- Cardenas, V.A., Reed, B., Chao, L.L., Chui, H., Sanossian, N., Decarli, C.C., Weiner, M.W., 2012. Associations among vascular risk factors, carotid atherosclerosis, and cortical volume and thickness in older adults. *Stroke* 43, 2865–2870.
- Chen, Z., Sun, J., Yang, Y., Lou, X., Wang, Y., Wang, Y., Ma, L., 2015. Cortical thinning in type 2 diabetes mellitus and recovering effects of insulin therapy. *J. Clin. Neurosci.* 22, 275–279.
- Chobanian, A.V., Bakris, G.L., Black, H.R., Cushman, W.C., Green, L.A., Izzo Jr., J.L., Roccella, E.J., 2003. Seventh report of the joint national committee on prevention, detection, evaluation, and treatment of high blood pressure. *Hypertension* 42, 1206–1252.
- Clerici, F., Caracciolo, B., Cova, I., Fusari Imperatori, S., Maggiore, L., Galimberti, D., Fratiglioni, L., 2012. Does vascular burden contribute to the progression of mild cognitive impairment to dementia? *Demen. Geriatr. Cogn. Disord.* 34, 235–243.
- De Toledo Ferraz Alves, T.C., Scazufca, M., Squarzon, P., De Souza Duran, F.L., Tamashiro-Duran, J.H., Vallada, H.P., Busatto, G.F., 2011. Subtle gray matter changes in temporo-parietal cortex associated with cardiovascular risk factors. *J. Alzheimers Dis.* 27, 575–589.
- Debetto, S., Seshadri, S., Beiser, A., Au, R., Himali, J.J., Palumbo, C., DeCarli, C., 2011. Midlife vascular risk factor exposure accelerates structural brain aging and cognitive decline. *Neurology* 77, 461–468.
- Devanand, D.P., Mikhno, A., Pelton, G.H., Cuasay, K., Pradhaban, G., Dileep Kumar, J.S., Parsey, R.V., 2010. Pittsburgh compound B (11C-PIB) and fluorodeoxyglucose (18 F-FDG) PET in patients with Alzheimer disease, mild cognitive impairment, and healthy controls. *J. Geriatr. Psychiatry Neurol.* 23, 185–198.
- Edison, P., Archer, H.A., Gerhard, A., Hinz, R., Pavese, N., Turkheimer, F.E., Brooks, D.J., 2008. Microglia, amyloid, and cognition in Alzheimer's disease: an [11C](R)PK11195-PET and [11C]PIB-PET study. *Neurobiol. Dis.* 32, 412–419.
- Fischl, B., Dale, A.M., 2000. Measuring the thickness of the human cerebral cortex from magnetic resonance images. *Proc. Natl. Acad. Sci. U S A* 97, 11050–11055.
- Gonzalez, C.E., Pacheco, J., Beason-Held, L.L., Resnick, S.M., 2015. Longitudinal changes in cortical thinning associated with hypertension. *J. Hypertens.* 33, 1242–1248.
- Haight, T.J., Bryan, R.N., Erus, G., Davatzikos, C., Jacobs, D.R., D'Esposito, M., Launer, L.J., 2015. Vascular risk factors, cerebrovascular reactivity, and the default-mode brain network. *Neuroimage* 115, 7–16.
- Hajjar, L., Zhao, P., Alsop, D., Novak, V., 2010. Hypertension and cerebral vasoreactivity: a continuous arterial spin labeling magnetic resonance imaging study. *Hypertension* 56, 859–864.
- He, Y., Chen, Z., Evans, A., 2008. Structural insights into aberrant topological patterns of large-scale cortical networks in Alzheimer's disease. *J. Neurosci.* 28, 4756–4766.
- Jack Jr., C.R., Bernstein, M.A., Fox, N.C., Thompson, P., Alexander, G., Harvey, D., Weiner, M.W., 2008. The Alzheimer's disease neuroimaging initiative (ADNI): MRI methods. *J. Magn. Reson. Imaging* 27, 685–691.
- Khedher, L., Ramirez, J., Górriz, J.M., Brahim, A., Segovia, F., 2015. Early diagnosis of Alzheimer's disease based on partial least squares, principal component analysis and support vector machine using segmented MRI images. *Neurocomputing* 151 (P1), 139–150.
- Kivipelto, M., Helkala, E.L., Hänninen, T., Laakso, M.P., Hallikainen, M., Alhainen, K., Nissinen, A., 2001. Midlife vascular risk factors and late-life mild cognitive impairment: a population-based study. *Neurology* 56, 1683–1689.
- Last, D., Alsop, D., Abduljalil, A., Marquis, R., de Bazelaire, C., Hu, K., Novak, V., 2007. Global and regional effects of type 2 diabetes on brain tissue volumes and cerebral vasoreactivity. *Diabetes Care* 30, 1193–1199.
- Leritz, E.C., Salat, D.H., Williams, V.J., Schnyer, D.M., Rudolph, J.L., Lipsitz, L., Milberg, W.P., 2011. Thickness of the human cerebral cortex is associated with metrics of cerebrovascular health in a normative sample of community dwelling older adults. *Neuroimage* 54, 2659–2671.
- Luchsinger, J.A., Reitz, C., Honig, L.S., Tang, M.X., Shea, S., Mayeux, R., 2005. Aggregation of vascular risk factors and risk of incident Alzheimer disease. *Neurology* 65, 545–551.
- Luk, G., Anderson, J.A.E., Craik, F.I.M., Grady, C., Bialystok, E., 2010. Distinct neural correlates for two types of inhibition in bilinguals: response inhibition versus interference suppression. *Brain Cogn.* 74, 347–357.
- Maillard, P., Carmichael, O.T., Reed, B., Mungas, D., DeCarli, C., 2015. Cooccurrence of vascular risk factors and late-life white-matter integrity changes. *Neurobiol. Aging* 36, 1670–1677.
- McIntosh, A.R., Bookstein, F.L., Haxby, J.V., Grady, C.L., 1996. Spatial pattern analysis of functional brain images using partial least squares. *Neuroimage* 3, 143–157.
- McIntosh, A.R., Chau, W.K., Protzner, A.B., 2004. Spatiotemporal analysis of event-related fMRI data using partial least squares. *Neuroimage* 23, 764–775.
- McIntosh, A.R., Lobaugh, N.J., 2004. Partial least squares analysis of neuroimaging data: applications and advances. *Neuroimage* 23 (Suppl. 1), S250–S263.
- McKhann, G., Drachman, D., Folstein, M., 1984. Clinical diagnosis of Alzheimer's disease: report of the NINCDS-ADRDA work group under the auspices of department of health and human services task force on Alzheimer's disease. *Neurology* 34, 939–944.
- McKhann, G.M., Knopman, D.S., Chertkow, H., Hyman, B.T., Jack Jr., C.R., Kawas, C.H., Phelps, C.H., 2011. The diagnosis of dementia due to Alzheimer's disease: recommendations from the National Institute on Aging-Alzheimer's Association workgroups on diagnostic guidelines for Alzheimer's disease. *Alzheimers Dement.* 7, 263–269.
- Murray, I.V.J., Proza, J.F., Sohrabji, F., Lawler, J.M., 2011. Vascular and metabolic dysfunction in Alzheimer's disease: a review. *Exp. Biol. Med.* 236, 772–782.
- Musen, G., Jacobson, A.M., Bolo, N.R., Simonson, D.C., Shenton, M.E., McCartney, R.L., Hoogenboom, W.S., 2012. Resting-state brain functional connectivity is altered in type 2 diabetes. *Diabetes* 61, 2375–2379.

- Nettiksimmons, J., DeCarli, C., Landau, S., Beckett, L., 2014. Biological heterogeneity in ADNI amnesic mild cognitive impairment. *Alzheimers Dement.* 10, 511–521.e1.
- Petersen, R.C., Smith, G.E., Waring, S.C., Ivnik, R.J., Tangalos, E.G., Kokmen, E., 1999. Mild cognitive impairment: clinical characterization and outcome. *Arch. Neurol.* 56, 303–308.
- Rondina, J.M., Squarzonni, P., Souza-Duran, F.L., Scazufca, M., Menezes, P.R., Vallada, H., Filho, G.B., 2014. Framingham coronary heart disease risk score can be predicted from structural brain images in elderly subjects. *Front. Aging Neurosci.* 6, 300.
- Sabuncu, M.R., Desikan, R.S., Sepulcre, J., Yeo, B.T.T., Liu, H., Schmansky, N.J., Fischl, B., 2011. The dynamics of cortical and hippocampal atrophy in Alzheimer disease. *Arch. Neurol.* 68, 1040–1048.
- Selby, J.V., Peng, T., Karter, A.J., Alexander, M., Sidney, S., Lian, J., Pettitt, D., 2004. High rates of co-occurrence of hypertension, elevated low-density lipoprotein cholesterol, and diabetes mellitus in a large managed care population. *Am. J. Manag. Care* 10, 163–170.
- Spulber, G., Simmons, A., Muehlboeck, J.S., Mecocci, P., Vellas, B., Tsolaki, M., Westman, E., 2013. An MRI-based index to measure the severity of alzheimer's disease-like structural pattern in subjects with mild cognitive impairment. *J. Intern. Med.* 273, 396–409.
- Tchistiakova, E., Crane, D.E., Mikulis, D.J., Anderson, N.D., Greenwood, C.E., Black, S.E., MacIntosh, B.J., 2015. Vascular risk factor burden correlates with cerebrovascular reactivity but not resting state coactivation in the default mode network. *J. Magn. Reson. Imaging* 42, 1369–1376.
- Thompson, P.M., Hayashi, K.M., De Zubicaray, G., Janke, A.L., Rose, S.E., Semple, J., Toga, A.W., 2003. Dynamics of gray matter loss in Alzheimer's disease. *J. Neurosci.* 23, 994–1005.
- van Velsen, E.F.S., Vermooij, M.W., Vrooman, H.A., van der Lugt, A., Breteler, M.M.B., Hofman, A., Ikram, M.A., 2013. Brain cortical thickness in the general elderly population: the Rotterdam Scan Study. *Neurosci. Lett.* 550, 189–194.
- Villeneuve, S., Reed, B.R., Madison, C.M., Wirth, M., Marchant, N.L., Kriger, S., Jagust, W.J., 2014. Vascular risk and A $\beta$  interact to reduce cortical thickness in AD vulnerable brain regions. *Neurology* 83, 40–47.
- Walhovd, K.B., Storsve, A.B., Westlye, L.T., Drevon, C.A., Fjell, A.M., 2014. Blood markers of fatty acids and vitamin D, cardiovascular measures, body mass index, and physical activity relate to longitudinal cortical thinning in normal aging. *Neurobiol. Aging* 35, 1055–1064.
- Zhao, L., Teter, B., Morihara, T., Lim, G.P., Ambegaokar, S.S., Ubeda, O.J., Cole, G.M., 2004. Insulin-degrading enzyme as a downstream target of insulin receptor signaling cascade: implications for Alzheimer's disease intervention. *J. Neurosci.* 24, 11120–11126.
- Zlokovic, B.V., 2011. Neurovascular pathways to neurodegeneration in Alzheimer's disease and other disorders. *Nat. Rev. Neurosci.* 12, X723–X738.